ESD-TR-68-216

A COMPUTER PROGRAM FOR PHYSICAL-OPTICS SCATTERING BY CONVEX CONDUCTING TARGETS - 2430-7

J.H. Richmond

May 1968

DEPUTY FOR SURVEILLANCE AND CONTROL SYSTEMS
ELECTRONIC SYSTEMS DIVISION
AIR FORCE SYSTEMS COMMAND
UNITED STATES AIR FORCE
L. G. Hanscom Field, Bedford, Massachusetts

(Prepared for Contract No. AF 19(628)-67-C-0308 by The Ohio State University, ElectroScience Laboratory, Department of Electrical Engineering, 1320 Kinnear Road, Columbus, Ohio.)

LEGAL NOTICE

OTHER NOTICES

ABSTRACT

This report describes a digital computer program which uses the physical optics approximation to calculate the scattering properties of convex perfectly conducting targets with arbitrary shape. The target shape is described in terms of the coordinates of a large number of points on the surface.

The program handles bistatic as well as backscattering problems. The input data specify the frequency, the incidence angles (θ_i, ϕ_i) and the scattering angles (θ_s, ϕ_s). In the CW case, the output data give the complex elements in the scattering matrix.

The program also handles the pulse case where the incident waveform has a finite number of cycles.

Graphs are included to illustrate typical results for the following target shapes: sphere, spheroids, ogive, and cone.

TABLE OF CONTENTS

A COMPUTER PROGRAM FOR PHYSICAL-OPTICS SCATTERING BY CONVEX CONDUCTING TARGETS

I. INTRODUCTION

Although the physical optics approximation for scattering by perfectly conducting targets has well-known limitations, it does provide rapid and efficient calculations which, in many cases, are reasonably accurate when the target is large in comparison with the wavelength.

In this report we present a digital computer program which uses the physical optics formulation to determine the scattering properties of perfectly conducting convex targets with arbitrary shape. Graphs are included to illustrate typical results for several target shapes.

The program is written in the Fortran IV language.

II. TARGET DESCRIPTION

The target shape is described in terms of the cartesian coordinates (x, y, z) of a large number of points on the surface. These points are selected on the intersections of the target surface and the planes $z = z_1$, $z = z_2$, etc. The coordinate origin is located in the interior of the target, and the surface is approximated by triangular facets with vertices at the given points. It is assumed that these points cover the surface with a density such that each facet is small in comparison with the wavelength. Experience indicates that reasonably good accuracy can be obtained with as few as 20 points per square wavelength on the target surface. The scattering data converge to the physical optics solution with approximately 80 points per square wavelength. Any further increase in the number of points will simply raise the conputational time.

When used with an IBM 7094 computer, the program will handle up to 1300 points. Magnetic tape or disk storage could be utilized to extend this capability.

The meter is used as the unit of length for the input data.

Punched cards are used for input data with the computer program. Figure 1 illustrates suitable input data for a prolate spheroidal target with major and minor axis lengths of 2 meters and 1 meter, respectively. The first input data card gives an integer N which specifies the number of planes $z = z_1$, $z = z_2$, ... $z = z_N$ employed to describe the target. The first line in Fig. 1 indicates that 30 planes are used for the spheroid. This first card is followed by N cards which list the z coordinates ZI(I) of these planes and the number of points NP(I) on each plane. These cards must be ordered with increasing values of the z coordinate. Thus, in Fig. 1, card 2 indicates that the first plane has $z = -1$ and there is only one point on this plane. Card 3 shows that the second plane is at $z = -0.98525$ and has 12 points. Finally, card 31 shows that the last plane is at $z = 1$ and has one point.

The remaining data cards (through 297) list the x and y coordinates of all the points on the target surface. These coordinates are given in pairs (x, y), with three pairs per card. For example, card 32 in Fig. 1 shows that the point on the first plane ($z = -1$) is at (0, 0). The next four cards (33-36) specify 12 points on the second plane, and card 297 locates the point on the last plane at (0, 0). The last cards (298-299) are described elsewhere in this report.

In the computer program, the coordinates x_k and y_k of point k on the plane $z = z_i$ are denoted by F(K) and G(K) or FP(K) and GP(K). The input data cards must give these points in an ordered manner, progressing in the clockwise direction (for a distant observer located on the negative z axis) around the contour on the plane $z = z_i$. Furthermore, the first given point on the plane $z = z_i$ should be the one nearest the first given point on the preceding plane.

The planes $z = z_i$ usually have unequal spacing. The spacing between these planes, and the number of points on each contour, should be designed to cover the target with a fairly uniform number of points per unit surface area.

The next section develops the physical-optics scattering equations used in the computer program.

III. THE PHYSICAL OPTICS FORMULATION

If the transmitting antenna is at a great distance from the target, it will illuminate the target with an incident field which is essentially a plane wave. In the CW case we let the time dependence $e^{j\omega t}$ be understood and represent the incident electric field intensity as follows:

$$(1) \qquad \underline{E}^i = (\hat{\theta}_i \, E_\theta^i + \hat{\phi}_i \, E_\phi^i) \, e^{jk \, \hat{r}_i \cdot \underline{r}}$$

```
      30                                                                   001
-1.00000          1                                                        002
-0.98525         12                                                        003
-0.94750         12                                                        004
-0.89425         16                                                        005
-0.83100         21                                                        006
-0.76175         24                                                        007
-0.68800         27                                                        008
(CARDS 9 THROUGH 24 ARE NOT SHOWN)
 0.68725         27                                                        025
 0.76100         24                                                        026
 0.83025         21                                                        027
 0.89350         16                                                        028
 0.94674         12                                                        029
 0.98449         12                                                        030
 1.00000          1                                                        031
 0.        0.                                                              032
 0.08556   0.         0.07410   0.04278   0.04278   0.07410               033
 0.00000   0.08556   -0.04278   0.07410  -0.07410   0.04278               034
-0.08556   0.00000   -0.07410  -0.04278  -0.04278  -0.07410               035
-0.00000  -0.08556    0.04278  -0.07410   0.07410  -0.04278               036
 0.15988   0.         0.13846   0.07994   0.07994   0.13846               037
 0.00000   0.15988   -0.07994   0.13846  -0.13846   0.07994               038
-0.15988   0.00000   -0.13846  -0.07994  -0.07994  -0.13846               039
-0.00000  -0.15988    0.07994  -0.13846   0.13846  -0.07994               040
 0.22378   0.         0.20675   0.08564   0.15824   0.15824               041
 0.08564   0.20675    0.00000   0.22378  -0.08564   0.20675               042
-0.15824   0.15824   -0.20675   0.08564  -0.22378   0.00000               043
-0.20675  -0.08564   -0.15824  -0.15824  -0.08564  -0.20675               044
-0.00000  -0.22378    0.08564  -0.20675   0.15824  -0.15824               045
 0.20675  -0.08564                                                         046
(CARDS 47 THROUGH 288 ARE NOT SHOWN)
 0.16099   0.         0.13942   0.08050   0.08050   0.13942               289
 0.00000   0.16099   -0.08050   0.13942  -0.13942   0.08050               290
-0.16099   0.00000   -0.13942  -0.08050  -0.08050  -0.13942               291
-0.00000  -0.16099    0.08050  -0.13942   0.13942  -0.08050               292
 0.08771   0.         0.07596   0.04385   0.04385   0.07596               293
 0.00000   0.08771   -0.04385   0.07596  -0.07596   0.04385               294
-0.08771   0.00000   -0.07596  -0.04385  -0.04385  -0.07596               295
-0.00000  -0.08771    0.04385  -0.07596   0.07596  -0.04385               296
 0.        0.                                                              297
    20.0         .0       20.0        .0                                   298
   300.0         20          3                                             299
```

Fig. 1. Typical input data for the computer program.

where (r_i, θ_i, ϕ_i) are the spherical coordinates of the transmitting antenna, $(\hat{r}_i, \hat{\theta}_i, \hat{\phi}_i)$ are the corresponding unit vectors,*

(2) $$k = 2\pi/\lambda ,$$

λ denotes the wavelength, and E^i_θ and E^i_ϕ are complex constants. An arbitrary point on the target surface is assigned the coordinates (r, θ, ϕ), the unit vectors $(\hat{r}, \hat{\theta}, \hat{\phi})$, and the position vector

(3) $$\underline{r} = r\,\hat{r}$$

Finally, the receiving antenna is assigned the coordinates (r_s, θ_s, ϕ_s) and the unit vectors $(\hat{r}_s, \hat{\theta}_s, \hat{\phi}_s)$. Thus θ_i and ϕ_i specify the incidence angles and θ_s and ϕ_s are the scattering angles. The magnetic field intensity of the incident plane wave is given by

(4) $$\underline{H}^i = (\hat{\theta}_i\, E^i_\phi - \hat{\phi}_i\, E^i_\theta)\,\frac{e^{jk\,\hat{r}_i \cdot \underline{r}}}{\eta}$$

where

(5) $$\eta = \sqrt{\mu/\epsilon} \quad .$$

The current density induced on the illuminated portion of the target surface is approximated as follows:

(6) $$\underline{J} = 2\hat{n} \times \underline{H}^i$$

---

* The unit vectors in the spherical system are related to those in the rectangular system by $\hat{r} = (\hat{x}x + \hat{y}y + \hat{z}z)/r$, $\hat{\phi} = -\hat{x}\sin\phi + \hat{y}\cos\phi$ and $\hat{r} \times \hat{\theta} = \hat{\phi}$.

where $\hat{n}$ denotes the outward unit normal vector on the surface. The vector potential for the distant scattered field is given by

$$(7) \qquad \underline{A} = \frac{\mu}{4\pi r_s} e^{-jkr_s} \iint \underline{J}\, e^{jk\hat{r}_s \cdot \underline{r}}\, ds \quad .$$

At a great distance from the target, the scattered field is

$$(8) \qquad \underline{E}^s = -j\omega \underline{A} = -\frac{j\omega\mu}{2\pi r_s} e^{-jkr_s} \iint \hat{n} \times \underline{H}^i e^{jk\hat{r}_s \cdot \underline{r}}\, ds \quad .$$

From Eqs. (4) and (8),

$$(9) \qquad \underline{E}^s = \frac{e^{-jkr_s}}{r_s} (\hat{\theta}_i E^i_\phi - \hat{\phi}_i E^i_\theta) \times \underline{S}$$

where

$$(10) \qquad \underline{S} = (j/\lambda) \iint \hat{n}\, e^{jk(\hat{r}_i + \hat{r}_s)\cdot \underline{r}}\, ds \quad .$$

The distant scattered field is represented by

$$(11) \qquad \underline{E}^s = (\hat{\theta}_s E^s_\theta + \hat{\phi}_s E^s_\phi) \frac{e^{-jkr_s}}{r_s}$$

where E^s_θ and E^s_ϕ denote complex constants. From Eqs. (9) and (11) and the following vector identity,

$$(12) \qquad \underline{A} \cdot (\underline{B} \times \underline{C}) = (\underline{A} \times \underline{B}) \cdot \underline{C} \ ,$$

it is found that

$$(13) \qquad E^s_\theta = (E^i_\theta \hat{\phi}_i \times \hat{\theta}_s + E^i_\phi \hat{\theta}_s \times \hat{\theta}_i) \cdot \underline{S}$$

and

$$E_\phi^s = (E_\theta^i \hat{\phi}_i \times \hat{\phi}_s + E_\phi^i \hat{\phi}_s \times \hat{\theta}_i) \cdot \underline{S} \quad . \tag{14}$$

It is convenient to define the CW scattering matrix as follows:

$$\begin{pmatrix} E_\theta^s \\ E_\phi^s \end{pmatrix} = \begin{pmatrix} S_{11} & S_{12} \\ S_{21} & S_{22} \end{pmatrix} \begin{pmatrix} E_\theta^i \\ E_\phi^i \end{pmatrix} \tag{15}$$

From Eqs. (13) through (15), the complex elements in the scattering matrix are given by

$$S_{11} = (\hat{\phi}_i \times \hat{\theta}_s) \cdot \underline{S} \tag{16}$$

$$S_{12} = (\hat{\theta}_s \times \hat{\theta}_i) \cdot \underline{S} \tag{17}$$

$$S_{21} = (\hat{\phi}_i \times \hat{\phi}_s) \cdot \underline{S} \tag{18}$$

$$S_{22} = (\hat{\phi}_s \times \hat{\theta}_i) \cdot \underline{S} \quad . \tag{19}$$

It is convenient to define a "vector area function" $\underline{A}(w)$ as follows:

$$\underline{S} = (j/\lambda) \int \underline{A}(w)\, e^{jkw}\, dw \quad , \tag{20}$$

where

$$w = (\hat{r}_i + \hat{r}_s) \cdot \underline{r} \tag{21}$$

It may be seen from Eq. (21) that w represents one of the coordinates of a point on the target surface, in a rectangular coordinate system that is rotated in space with respect to the (x, y, z) system. The w axis is coplanar with $\hat{r}_i$ and $\hat{r}_s$ and bisects the angle between these unit vectors. The unit of length for the w coordinate generally differs from that for x, y, and z.

For any point (x, y, z) on the target surface,

$$w = (\sin\theta_i \cos\phi_i + \sin\theta_s \cos\phi_s)x + (\sin\theta_i \sin\phi_i + \sin\theta_s \sin\phi_s)y + (\cos\theta_i + \cos\theta_s)z \quad . \tag{22}$$

Once the vector area function has been calculated, $\underline{S}$ can be determined efficiently from Eq. (20) by numerical integration. Equation (10) would take more computation time since it involves a surface integral instead of a line integral.

Once $\underline{S}$ has been calculated, the elements in the scattering matrix are determined as follows:

$$S_{11} = S_x X_{11} + S_y Y_{11} + S_z Z_{11} \tag{23}$$

$$S_{12} = S_x X_{12} + S_y Y_{12} + S_z Z_{12} \tag{24}$$

$$S_{21} = S_z Z_{21} \tag{25}$$

$$S_{22} = S_x X_{22} + S_y Y_{22} + S_z Z_{22} \tag{26}$$

where

$$\underline{S} = \hat{x} S_x + \hat{y} S_y + \hat{z} S_z \tag{27}$$

$$X_{11} = -\cos\phi_i \sin\theta_s \tag{28}$$

$$Y_{11} = -\sin\phi_i \sin\theta_s \tag{29}$$

$$Z_{11} = -(\sin\phi_i \sin\phi_s + \cos\phi_i \cos\phi_s) \cos\theta_s \tag{30}$$

$$X_{12} = \cos\theta_i \sin\phi_i \sin\theta_s - \sin\theta_i \cos\theta_s \sin\phi_s \tag{31}$$

(32) $Y_{12} = \sin\theta_i \cos\theta_s \cos\phi_s - \cos\theta_i \cos\phi_i \sin\theta_s$

(33) $Z_{12} = (\sin\phi_i \cos\phi_s - \cos\phi_i \sin\phi_s) \cos\theta_i \cos\theta_s$

(34) $Z_{21} = \cos\phi_i \sin\phi_s - \sin\phi_i \cos\phi_s$

(35) $X_{22} = - \sin\theta_i \cos\phi_s$

(36) $Y_{22} = - \sin\theta_i \sin\phi_s$

(37) $Z_{22} = - (\cos\phi_i \cos\phi_s + \sin\phi_i \sin\phi_s) \cos\theta_i \quad .$

In the pulse case, the incident wave is considered to have M complete cycles and a square modulation envelope. M is assumed to be an integer, and the incident field is expressed by

(38) $$\underline{E}^i = (\hat{\theta}_i E_\theta^i + \hat{\phi}_i E_\phi^i) \sin(\omega t + k \hat{r}_i \cdot \underline{r})$$
$$\cdot \left[u(\omega t + k \hat{r}_i \cdot \underline{r}) - u(\omega t + k \hat{r}_i \cdot \underline{r} - \omega \tau) \right]$$

where E_θ^i and E_ϕ^i are real constants, u(x) denotes the unit step function, f is the carrier frequency,

(39) $\omega = 2\pi f \quad ,$

(40) $T = 1/f \quad ,$

and

(41) $\tau = MT \quad .$

The scattered field is given by

$$(42) \qquad \underline{E}^s(r_s, t) = [\hat{\theta}_s \, E^s_\theta(t - r_s/c) + \hat{\phi}_s \, E^s_\phi(t - r_s/c)] \, \frac{1}{r_s} \quad ,$$

where c denotes the speed of light in free space.

It is convenient to write the following matrix equation

$$(43) \qquad \begin{pmatrix} E^s_\theta(t) \\ E^s_\phi(t) \end{pmatrix} = \begin{pmatrix} F_{11}(t) & F_{12}(t) \\ F_{21}(t) & F_{22}(t) \end{pmatrix} \begin{pmatrix} E^i_\theta \\ E^i_\phi \end{pmatrix} \quad .$$

The pulse response of the target is thus defined with four functions of time given by

$$(44) \qquad F_{11}(t) = (\hat{\phi}_i \times \hat{\theta}_s) \cdot \underline{F}(t)$$

$$(45) \qquad F_{12}(t) = (\hat{\theta}_s \times \hat{\theta}_i) \cdot \underline{F}(t)$$

$$(46) \qquad F_{21}(t) = (\hat{\phi}_i \times \hat{\phi}_s) \cdot \underline{F}(t)$$

$$(47) \qquad F_{22}(t) = (\hat{\phi}_s \times \hat{\theta}_i) \cdot \underline{F}(t)$$

where

$$(48) \qquad \underline{F}(t) = \frac{1}{\lambda} \int \int \hat{n} \cos(\omega t + kw) \cdot [u(\omega t + kw) - u(\omega t + kw - \omega\tau)] \, ds$$

Equation (48) can also be written as follows

$$(49) \qquad \underline{F}(t) = \frac{1}{\lambda} \int \underline{A}(w) \cos(\omega t + kw) \, [u(\omega t + kw) - u(\omega t + kw - \omega\tau)] \, dw \quad .$$

Equation (49) is employed in the computer program since it permits more rapid calculations than Eq. (48).

The scattering waveforms $F_{11}(t)$, $F_{12}(t)$, $F_{21}(t)$ and $F_{22}(t)$ are calculated at a discrete set of equally spaced points in time. The spacing between these points is determined by an integer L, included in the input data, as follows

$$\Delta T = T/L \quad . \tag{50}$$

The first and last points coincide with the initiation and the termination of the pulse response.

It must be noted that the above formulation for the pulse response assumes the incident plane wave has linear polarization. However, it appears that the more general situation could be programmed quite readily.

The physical-optics scattering program is described in some detail in the following sections.

IV. APPROXIMATING THE TARGET WITH A POLYHEDRON

Figure 2 shows the first 91 statements or cards in the computer program. Card 26 reads the integer N which specifies the number of planes used in describing the target surface. Card 29 reads the z coordinate ZI(I) for each of these planes and the number of points NP(I) on each plane. The dimension statements reserve core storage for 200 planes, 500 points on each plane, and a total of 1300 points.

Card 37 reads the x and y coordinates of the points on the first plane, and card 48 reads the coordinates of the remaining points.

In addition to reading the target description, this first section of the program sets up a polyhedral approximation for the target. This polyhedron has many triangular facets, with vertices at the given points. If each facet is small in comparison with the wavelength, the scattering properties of the polyhedron will be nearly the same as for the real target of interest.

```
$EXECUTE          IBJOB
$IBJOB            MAP
$IBFTC PHYSOP   NODECK
   21   FORMAT(1X,8E15.7)
   22   FORMAT(1X,8F15.7)
   23   FORMAT(1H0)
   24   FORMAT(1X,10F12.4)
   25   FORMAT(8F9.3)
   26   FORMAT(7F10.5)
   27   FORMAT(7I10)
   28   FORMAT(1H1)
   29   FORMAT(1F10.5,6I10)
   31   FORMAT(1X,7H   THI =,F10.4,7H   PHI =,F10.4,7H   THS =,F10.4,
       27H   PHS =,F10.4/)
   32   FORMAT(1X,5HFMC =,F10.4,8H   WAVE =,F15.7/)
   33   FORMAT(1X,5HS11 =,2F15.7,7H   S12 =,2F15.7,7H   S21 =,2F15.7/
       27H   S22 =,2F15.7/)
   34   FORMAT(1X,6HEA11 =,F15.7,8H   EA12 =,F15.7,8H   EA21 =,F15.7,8H   EA2
       22 =,F15.7/)
        DIMENSION AX(500),AY(500),AZ(500)
        DIMENSION X(2600),Y(2600),Z(2600),XN(2600),YN(2600),ZN(2600)
        DIMENSION F(500),G(500),FP(500),GP(500),ZI(200),NP(200)
        COMPLEX SX,SY,SZ,S11,S12,S21,S22,QA,QB,QC,QD,QK,QL
        DATA TP,FP1,RAD/6.2831853,12.56637,.01745329/
    1   J=0
        READ(5,27)N
        WRITE(6,27)N
        DO 60 I=1,N
   60   READ(5,29)ZI(I),NP(I)
        FN=N
        M=NP(1)
        MM=M+1
        ZA=ZI(1)
        NC=(M+2)/3
        DO 80 I=1,NC
        K=3*I-2
   80   READ(5,26)F(K),G(K),F(K+1),G(K+1),F(K+2),G(K+2)
        F(MM)=F(1)
        G(MM)=G(1)
        IF(M.EQ.1) MM=1
        DO 150 II=2,N
        MP=NP(II)
        MPP=MP+1
        ZC=ZI(II)
        NC=(MP+2)/3
        DO 90 I=1,NC
        K=3*I-2
   90   READ(5,26)FP(K),GP(K),FP(K+1),GP(K+1),FP(K+2),GP(K+2)
        FP(MPP)=FP(1)
        GP(MPP)=GP(1)
        IF(MP.EQ.1) MPP=1
        L=1
        LP=1
   95   XA=F(L)
        XC=FP(LP)
        YA=G(L)
        YC=GP(LP)
        J=J+1
        IF(L.EQ.MM) GO TO 98
        IF(LP.EQ.MPP) GO TO 100
        RA=(FP(LP+1)-F(L))**2+(GP(LP+1)-G(L))**2
```

Fig. 2. First section of the computer program.

```
      RB=(FP(LP)-F(L+1))**2+(GP(LP)-G(L+1))**2
      IF(RA.GT.RB) GO TO 100
98    LP=LP+1
      XB=FP(LP)
      YB=GP(LP)
      ZB=ZC
      GO TO 110
100   L=L+1
      XB=F(L)
      YB=G(L)
      ZB=ZA
110   X(J)=(XA+XB+XC)/3.
      Y(J)=(YA+YB+YC)/3.
      Z(J)=(ZA+ZB+ZC)/3.
      XN(J)=((YB-YA)*(ZC-ZA)-(ZB-ZA)*(YC-YA))*.5
      YN(J)=((ZB-ZA)*(XC-XA)-(XB-XA)*(ZC-ZA))*.5
      ZN(J)=((XB-XA)*(YC-YA)-(YB-YA)*(XC-XA))*.5
      IF(L.LT.MM.OR.LP.LT.MPP) GO TO 95
      DO 120 I=1,MPP
      F(I)=FP(I)
120   G(I)=GP(I)
      M=MP
      MM=MPP
      ZA=ZC
150   CONTINUE
      NT=J
      DZ=.0
      DO 155 I=2,N
      DEL=ZI(I)-ZI(I-1)
155   IF(DEL.GT.DZ)DZ=DEL
```

Fig. 2. First section of the computer program. (cont.)

Since each facet is assumed to be small, the only parameters that must be determined and stored for each one are its vector area and the coordinates of its midpoint.

Each triangle is assigned an index number denoted by J. The coordinates of a point at the center of triangle J are denoted by X(J), Y(J) and Z(J). The cartesian components of the vector area (using the outward normal direction) of triangle J are XN(J), YN(J) and ZN(J). The dimension statements reserve core storage for these parameters for 2600 triangular facets. The number of triangles is approximately twice the number of points on the target surface, and is denoted by NT.

The technique for fitting a polyhedron to a given array of points is illustrated in Fig. 3. The computer first processes all the triangular facets on the first "zone" of the surface (i.e., the portion of

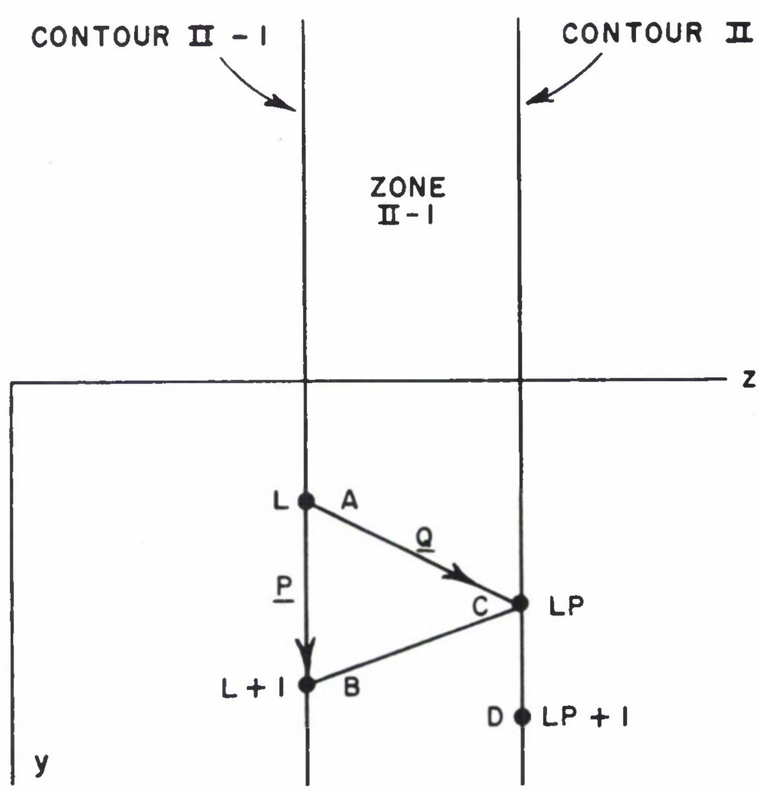

Fig. 3. A typical triangular facet on the polyhedron.

the surface bounded by the first two planes $z = z_1$ and $z = z_2$). It then proceeds to the next zone. In the situation illustrated in Fig. 3, the computer is identifying and processing the triangles in Zone II-1. The x and y coordinates of the points on contour II-1 are denoted by F and G, and those on contour II by FP and GP. The first triangle on this zone has one vertex at the point x = F(1), y = G(1) and z = ZI(II-1). Another vertex is at x = FP(1), y = GP(1) and z = ZI(II). The third vertex of this first triangle is at (F(2), G(2)) or (FP(2), GP(2)), whichever yields the "most compact" triangle.

When the computer has completed the processing of a given triangle in a given zone, two vertices on the next triangle are predetermined since they coincide with two of the vertices on the last completed triangle. In Fig. 3, these two vertices are indicated by points A and C. Point A is the L-th point on contour II-1 and its coordinates are XA=F(L), YA= G(L) and ZA = ZI(II-1). Point C is the LP-th point on contour II and its coordinates are XC = FP(LP), YC = GP(LP) and ZC = ZI(II). To establish the third point on the triangle, the computer compares the lengths of the lines AD and BC and selects the shorter one to form one side of the triangle. As shown in Fig. 3, B denotes the (L+1)-th point on contour II-1, and D is the (LP+1)-th point on contour II.

For the situation shown in Fig. 3, BC is shorter than AD. Therefore, B is selected as the third vertex of the triangle and assigned the following coordinates: XB = F(L+1), YB = G(L+1) and ZB = ZA. The coordinates of the midpoint of this triangle are calculated in cards 73, 74 and 75. The vector area of the triangle is given by $(\underline{P} \times \underline{Q})/2$, where the vector $\underline{P}$ extends from A to B and the vector $\underline{Q}$ extends from A to C. This calculation is arranged by cards 76, 77 and 78 to determine the rectangular components of the vector area.

Having completed the processing of triangle J, the computer proceeds with the next triangle in a similar fashion.

When the computer finishes the first section of the program, it has in storage a complete list of the midpoint coordinates and the vector areas of all of the triangular facets on the polyhedron.

V. COMPUTING THE VECTOR AREA FUNCTION

The second section of the computer program reads the coordinates (θ_i, ϕ_i) of the transmitting antenna and (θ_s, ϕ_s) of the receiving antenna and calculates the corresponding vector area function $\underline{A}(w)$ for the target. This part of the program is shown in Fig. 4.

Card 92 reads $\theta_i, \phi_i, \theta_s$ and ϕ_s. These angles are denoted by THI, PHI, THS and PHS. They must be given in degrees (rather than radians) in the input data. For example, card 298 in Fig. 1 assigns a value of 20 degrees for θ_i and θ_s, and zero degrees for ϕ_i and ϕ_s.

In the DO LOOP in cards 115 through 137, the computer scans the w coordinates for all the illuminated facets on the polyhedron to determine the maximum and minimum values of w on the illuminated portion of the target surface. These are designated WMAX and WMIN. WX, WY and WZ represent the coefficients of x, y and z in Eq. (22).

Cards 138 through 147 calculate the coefficients X_{11}, Y_{11}, etc., defined by Eqs. (28) through (37).

The rectangular components of the vector area function $\underline{A}(w)$ are denoted by AX(K), AY(K) and AZ(K). The program is designed to calculate several values of AX, AY and AZ, representing samples of the functions for uniformly spaced points on the w axis. The dimension statements allow for a maximum of 500 sampling points. The area function is nonzero only for values of w between WMIN and WMAX. Therefore, this portion of the w axis is divided into KX segments and the sampling points are selected at the centers of these segments. Thus, AX(1), AY(1) and AZ(1) represent the components of $\underline{A}(w)$ at the center of the first segment (i.e., the segment which begins at WMIN). Likewise, AX(KX), AY(KX) and AZ(KX) represent the components of $\underline{A}(w)$ at the center of the last segment (which terminates at WMAX). The length of each segment (and the spacing between the sampling points) is denoted by DEL. WI and WF denote the values of w at the first and last sampling points.

If the number of sampling points is too small, the area function will not be represented adequately and one cannot expect accurate scattering data. Therefore, the program always calculates the largest number of samples consistent with the input data. To obtain a more detailed area function for a given target, one simply supplies a more detailed description of the target via the input data.

The following expression for the vector area function can be obtained by comparing Eqs. (10) and (20):

(51) $$\underline{A}(w) = \frac{d}{dw} \int\int \hat{n} \, ds \quad .$$

The significance of Eq. (51) can be clarified by considering the equivalent finite-difference approximation:

(52) $$\underline{A}(K) = \frac{1}{DEL} \int\int_{S_k} \hat{n} \, ds \quad ,$$

where $\underline{A}(K)$ represents the area function at the point $w = w_k$ and S_k denotes a narrow zone on the illuminated portion of the target surface bounded by the planes $w = w_k - DEL/2$ and $w = w_k + DEL/2$.

For the polyhedron with small facets, Eq. (52) takes the following form:

(53) $$\underline{A}(K) = \sum \frac{\hat{x}\, XN(I) + \hat{y}\, YN(I) + \hat{z}\, ZN(I)}{DEL}$$

The summation indicated in Eq. (53) is programmed in cards 162 through 199 in Fig. 4. In Eq. (53) it is understood that the summation extends only over the illuminated facets with w coordinates in the range $w_k \pm DEL/2$.

A simple shadowing test is programmed in cards 163 and 164. RDTN represents the quantity $\hat{r}_i \cdot \hat{n}$. RDTN is calculated for each facet on the polyhedron. The facet is considered illuminated or shadowed according as RDTN is positive or negative. This test is, of course, adequate only for convex targets.

Figure 5 shows the vector area components AX(w) and AZ(w) for a prolate spheroid. AY(w) is zero for this problem. The input data in Fig. 1 were used for these calculations.

Although independent data are not available for comparison with the curves in Fig. 5, there are two indications that these curves are reliable. First, these area functions lead to accurate physical-optics scattering data. Second, the area functions calculated in the same manner show close agreement with known results for the following cases: backscatter and bistatic scattering from spheres and axial backscatter from spheroids, ogives and cones.

```
2     READ(5,26)THI,PHI,THS,PHS
      WRITE(6,31)THI,PHI,THS,PHS
      STHI=SIN(RAD*THI)
      CTHI=COS(RAD*THI)
      STHS=SIN(RAD*THS)
      CTHS=COS(RAD*THS)
      SPHI=SIN(RAD*PHI)
      CPHI=COS(RAD*PHI)
      SPHS=SIN(RAD*PHS)
      CPHS=COS(RAD*PHS)
      SSCS=STHS*CPHS
      SSSS=STHS*SPHS
      SICI=STHI*CPHI
      SISI=STHI*SPHI
      WX=SICI+SSCS
      WY=SISI+SSSS
      WZ=CTHI+CTHS
      DEL=DZ*SQRT(WX**2+WY**2+WZ**2)
      WMAX=-1000000.
      WMIN=1000000.
      K=2
      ZA=ZI(1)
      ZC=ZI(2)
      DO 200 I=1,NT
      RDTN=XN(I)*SICI+YN(I)*SISI+ZN(I)*CTHI
      IF(RDTN.LE.0.) GO TO 200
      ZNI=ZN(I)
      ZB=Z(I)
      IF(ZC.GE.ZB)GO TO 170
165   K=K+1
      ZA=ZI(K-1)
      ZC=ZI(K)
      IF(ZC.LT.ZB)GO TO 165
170   DEN=X(I)*XN(I)+Y(I)*YN(I)
      D=DEN+ZB*ZNI
      F=(D-ZA*ZNI)/DEN
      WA=X(I)*F*WX+Y(I)*F*WY+ZA*WZ
      F=(D-ZC*ZNI)/DEN
      WC=X(I)*F*WX+Y(I)*F*WY+ZC*WZ
      IF(WC.GE.WA)GO TO 175
      WW=WA
      WA=WC
      WC=WW
175   IF(WC.GT.WMAX)WMAX=WC
      IF(WA.LT.WMIN)WMIN=WA
200   CONTINUE
      X11=-CPHI*STHS
      Y11=-SPHI*STHS
      Z11=-(SPHI*SPHS+CPHI*CPHS)*CTHS
      X12=CTHI*SPHI*STHS-STHI*CTHS*SPHS
      Y12=STHI*CTHS*CPHS-CTHI*CPHI*STHS
      Z12=(-CPHI*SPHS+SPHI*CPHS)*CTHI*CTHS
      Z21=-SPHI*CPHS+CPHI*SPHS
      X22=-STHI*CPHS
      Y22=-STHI*SPHS
      Z22=-(CPHI*CPHS+SPHI*SPHS)*CTHI
      DO 205 K=1,500
      AX(K)=0.0
      AY(K)=0.0
205   AZ(K)=0.0
      KX=(WMAX-WMIN)/DEL
```

Fig. 4. Second section of the computer program.

```
      FK=KX
      DEL=(WMAX-WMIN)/FK
      WRITE(6,22)DZ,DEL,WMIN,WMAX
      DELT=DEL/2.
      WI=WMIN+DELT
      WF=WMAX-DELT
      K=2
      ZA=ZI(1)
      ZC=ZI(2)
      DO 230 I=1,NT
      RDTN=XN(I)*SICI+YN(I)*SISI+ZN(I)*CTHI
      IF(RDTN.LE.0.) GO TO 230
      ZNI=ZN(I)
      ZB=Z(I)
      IF(ZC.GE.ZB)GO TO 215
  210 K=K+1
      ZA=ZI(K-1)
      ZC=ZI(K)
      IF(ZC.LT.ZB)GO TO 210
  215 DEN=X(I)*XN(I)+Y(I)*YN(I)
      D=DEN+ZB*ZNI
      F=(D-ZA*ZNI)/DEN
      WA=X(I)*F*WX+Y(I)*F*WY+ZA*WZ
      F=(D-ZC*ZNI)/DEN
      WC=X(I)*F*WX+Y(I)*F*WY+ZC*WZ
      IF(WC.GE.WA)GO TO 218
      WW=WA
      WA=WC
      WC=WW
  218 KA=(WA-WI)/DEL+1.5
      KC=(WC-WI)/DEL+1.5
      IF(KA.NE.KC)GO TO 220
      AX(KA)=AX(KA)+XN(I)
      AY(KA)=AY(KA)+YN(I)
      AZ(KA)=AZ(KA)+ZN(I)
      GO TO 230
  220 FKA=KA-1
      W=FKA*DEL+WI+DELT
      D=(W-WA)/(WC-WA)
      AX(KA)=AX(KA)+XN(I)*D
      AY(KA)=AY(KA)+YN(I)*D
      AZ(KA)=AZ(KA)+ZN(I)*D
      F=1.-D
      AX(KC)=AX(KC)+XN(I)*F
      AY(KC)=AY(KC)+YN(I)*F
      AZ(KC)=AZ(KC)+ZN(I)*F
  230 CONTINUE
      W=WI
      DO 235 K=1,KX
      AX(K)=AX(K)/DEL
      AY(K)=AY(K)/DEL
      AZ(K)=AZ(K)/DEL
      FK=K
      WRITE(6,22) FK,W,AX(K),AY(K),AZ(K)
  235 W=W+DEL
      AX(KX+1)=2.*AX(KX)-AX(KX-1)
      AY(KX+1)=2.*AY(KX)-AY(KX-1)
      AZ(KX+1)=2.*AZ(KX)-AZ(KX-1)
      WRITE (6,23)
```

Fig. 4. Second section of the computer program. (cont.)

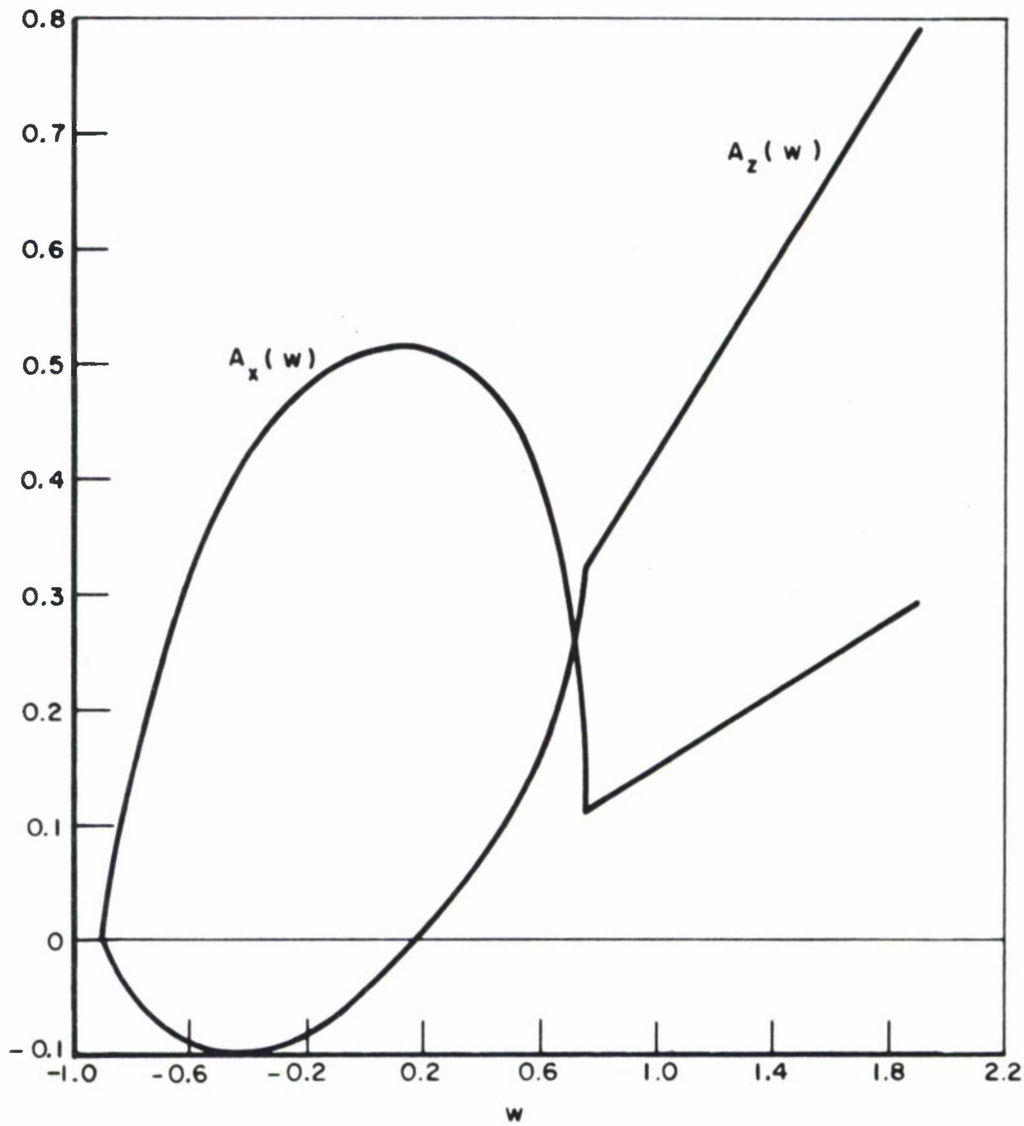

Fig. 5. Calculated area functions for a prolate spheroid using input data from Fig. 1.

VI. COMPUTING THE CW SCATTERING MATRIX

The third section of the computer program, shown in Fig. 6, reads the frequency in megahertz and calculates the CW scattering matrix and the corresponding echo areas. In addition to the frequency, card 212 also reads the integers L and M which are defined in the next section. L and M are not needed for the CW calculations and could just as well be read later at card 249. Suitable input data for card 212 are shown in card 299 in Fig. 1.

This section of the program calculates the vector $\underline{S}$ defined by

$$(54) \qquad \underline{S} = (j/\lambda) \int_{wmin}^{wmax} \underline{A}(w) \; e^{jkw} \; dw \quad .$$

The integral in Eq. (54) is evaluated with the "piecewise linear method" described in Reference 1. We integrate over segment k on the w axis and then sum on k. Segment k has length DEL and is centered at $w = w_k$. On segment k a straight-line approximation is used for the area function:*

$$(55) \qquad \underline{A}(w) = \underline{a}_k + \underline{b}_k \, w \quad .$$

By fitting Eq. (55) to the stored samples $\underline{A}(K)$ at w_k and $\underline{A}(K+1)$ at w_{k+1}, we find that

$$(56) \qquad \underline{a}_k = [\, \underline{A}(K) \, w_{k+1} - \underline{A}(K+1) \, w_k] / DEL$$

and

$$(57) \qquad \underline{b}_k = [\, \underline{A}(K+1) - \underline{A}(K)] / DEL \quad .$$

---

* When k is used as a subscript it represents the index of a segment on the w axis and is denoted in the program by K. When used otherwise, as in Eqs. (54) and (59), k is defined by Eq. (2) and is denoted in the program by TPL.

The integration in Eq. (54) can be performed analytically when $\underline{A}(w)$ is given by Eq. (55). This leads to the following expression

$$(58) \qquad \underline{S} = \frac{1}{2\pi\, DG} \sum_{k=1}^{KX} \left[QK\, \underline{A}(K) + QL\, \underline{A}(K+1) \right] \quad ,$$

where

$$(59) \qquad DG = k\ DEL \ ,$$

$$(60) \qquad QK = (GL - j)\ QD - QC \quad ,$$

$$(61) \qquad QL = QC - (GK - j)\ QD \quad ,$$

$$(62) \qquad QC = GB\ e^{j\ GB} - GA\ e^{j\ GA} \quad ,$$

$$(63) \qquad QD = e^{j\ GB} - e^{j\ GA} \quad ,$$

$$(64) \qquad GA = k(w_k - DEL/2) \quad ,$$

$$(65) \qquad GB = k(w_k + DEL/2) \quad ,$$

$$(66) \qquad GK = k\ w_k \quad ,$$

and

$$(67) \qquad GL = k\ w_{k+1} \quad .$$

The summation in Eq. (58) is programmed in cards 223 through 236. The rectangular components of $\underline{S}$ are denoted by SX, SY and SZ.

Equations (23) - (26) are programmed in cards 238 - 241 to calculate the complex elements in the scattering matrix. This scattering matrix is the principal output of this section of the program. With it available, one can use Eq. (15) to calculate the scattering properties of the target for any given incident polarization.

The remaining output from this section does not necessarily have any significance except in special cases. In backscatter problems, however, EA11 represents the echo area in square meters. Furthermore, EA11 and EA22 represent the E-plane and H-plane echo areas when $\phi_i = \phi_s$ and the target has axial symmetry with respect to the z axis.

Using the techniques described above and the input data shown in Fig. 1, the computer yields the following CW scattering data for the prolate spheroid at 300 MHz:

S11 = S22 = -0.1191 + j 0.0637

S12 = S21 = 0

EA11 = EA22 = 0.229

EA12 = EA21 = 0

Although the piecewise-linear integration technique is efficient and successful for most problems, it is not appropriate in forward scattering problems (where w = 0 everywhere on the target) or in specular scattering from a flat region on the target (where w is constant over a significant portion of the surface). Therefore, the computer output data are not reliable in these cases.

VII. COMPUTING THE PULSE RESPONSE

The pulse scattering problem is treated in the fourth and last section of the program shown in Fig. 7. The entire program is ready for the computer when the four sections are put together (with the card numbers running sequentially from 1 through 345) and backed up with suitable input data (such as cards 1 through 299 in Fig. 1).

To explain the pulse calculations, it is convenient to write Eq. (49) in the following form

```
3     READ(5,29)FMC,L,M
      WAVE=299.79/FMC
      WRITE(6,32) FMC,WAVE
      TPL=TP/WAVE
      SX=(.0,.0)
      SY=(.0,.0)
      SZ=(.0,.0)
      GK=TPL*W1
      GA=TPL*WMIN
      DG=TPL*DEL
      QA=CMPLX(COS(GA),SIN(GA))
      DO 240 K=1,KX
      GB=GA+DG
      QB=CMPLX(COS(GB),SIN(GB))
      GL=GK+DG
      QC=GB*QB-GA*QA
      QD=QB-QA
      QK=QD*GL-QC-(.0,1.)*QD
      QL=QC-QD*GK+(.0,1.)*QD
      SX=SX+QK*AX(K)+QL*AX(K+1)
      SY=SY+QK*AY(K)+QL*AY(K+1)
      SZ=SZ+QK*AZ(K)+QL*AZ(K+1)
      GA=GB
      GK=GL
240   QA=QB
      DEN=TP*DG
      S11=(SX*X11+SY*Y11+SZ*Z11)/DEN
      S12=(SX*X12+SY*Y12+SZ*Z12)/DEN
      S21=SZ*Z21/DEN
      S22=(SX*X22+SY*Y22+SZ*Z22)/DEN
      WRITE(6,33) S11,S12,S21,S22
      EA11=(CABS(S11)**2)*FPI
      EA12=(CABS(S12)**2)*FPI
      EA21=(CABS(S21)**2)*FPI
      EA22=(CABS(S22)**2)*FPI
      WRITE(6,34) EA11,EA12,EA21,EA22
      WRITE (6,23)
```

Fig. 6. Third section of the computer program.

(68) $$\underline{F}(t) = \frac{1}{2\pi}\left[\cos \omega t \int_{x_a}^{y_a} \underline{A}(g) \cos g \, dg - \sin \omega t \int_{x_a}^{y_a} \underline{A}(g) \sin g \, dg\right] ,$$

where

(69) $$g = kw \quad ,$$

(70) $$x_a = GN \text{ or } -\omega t \text{ (whichever is larger)} \quad ,$$

(71) $$y_a = GX \text{ or } \omega_T - \omega t \text{ (whichever is smaller)} \quad ,$$

(72) $$GN = k \; WMIN,$$

and

(73) $$GX = k \; WMAX \quad .$$

The area function $\underline{A}(g)$ is the same as $\underline{A}(w)$, and it has already been calculated and stored in AX(K), AY(K) and AZ(K).

The integer L determines the number of points per cycle to be calculated on the scattering waveforms. Card 254 calculates the size of the increments in ωt as follows:

(74) $$DWT = 2\pi/L \quad .$$

The integer M specifies the number of complete cycles in the incident waveform. The pulse width of the incident waveform, as measured in radians and observed at an arbitrary point in space, is calculated by card 253 as follows:

(75) $$\omega_T = WTAU = 2\pi M \quad .$$

The scattering function $\underline{F}(t)$ is nonzero only in the following interval: $-GX < \omega t < \omega_T - GN$.

It is convenient to assign symbols to the integrals in Eq. (68) as follows:

$$\underline{U}(t) = \int_{x_a}^{y_a} \underline{A}(g) \cos g \, dg, \tag{76}$$

and

$$\underline{V}(t) = \int_{x_a}^{y_a} \underline{A}(g) \sin g \, dg \quad . \tag{77}$$

These are functions of time by virtue of the time dependent limits x_a and y_a. In the program the rectangular components of $\underline{U}(t)$ are denoted by UX, UY and UZ, and the components of $\underline{V}(t)$ are VX, VY and VZ. WT, SWT and CWT denote ωt, $\sin \omega t$ and $\cos \omega t$.

$\underline{U}(t)$ and $\underline{V}(t)$ are identically zero for all values of ωt less than or equal to $-$ GX. Thus, the computer begins the pulse-response calculations by setting $\omega t = -$ GX (card 261), initializing $\underline{U}(t)$ and $\underline{V}(t)$ to zero (cards 269 - 274) and writing out the first data point on the scattering waveform (card 268). At this point in time, the integration limits are found from Eqs. (70) and (71) to be $x_a = y_a =$ GX.

Suppose the computer has just completed the calculation of the scattering data for a given value of ωt, has incremented ωt in card 277, and is preparing to calculate the next point on the scattering waveform. The first step in the procedure is to determine the integration limits x_a and y_a, denoted by XA and YA. This is accomplished in cards 281 - 292 in accordance with Eqs. (70) and (71). These cards also determine the indices KA and LA of the segments on the g axis which contain the points g = XA and g = YA, respectively.

The integrals $\underline{U}(t')$ and $\underline{V}(t')$ currently in storage have limits now denoted by XB and YB by virtue of cards 338 and 339. Since XA and YA are equal to or less than XB and YB, respectively,

$$\underline{U}(t) = \underline{U}(t') + \int_{XA}^{XB} \underline{A}(g) \cos g \, dg - \int_{YA}^{YB} \underline{A}(g) \cos g \, dg \tag{78}$$

and

$$(79) \qquad \underline{V}(t) = \underline{V}(t') + \int_{XA}^{XB} \underline{A}(g) \sin g \, dg - \int_{YA}^{YB} \underline{A}(g) \sin g \, dg \quad .$$

Calculations based on Eqs. (78) and (79) are, of course, far more efficient than Eqs. (76) and (77).

Equations (78) and (79) are programmed in cards 294 - 329. The piecewise-linear technique is employed to evaluate the integrals in these equations. The integrals with limits XA and XB are evaluated in the first pass through the DO LOOP that begins with card 299, and those with limits YA and YB are calculated in the second pass. In each pass, ZA and ZB denote the limits of integration. Initially I denotes the index number of the g-axis segment containing the point g = ZA and G is the value of g at the center of this segment. $\underline{A}(g)$ is treated as a linear function over this segment in the same manner as in Eqs. (55) through (57). GP denotes the value of g at the center of segment I + 1, and HA and HB are the limits of the subintegral on segment I. When the integration on segment I is finished, the computer moves on to the next segment (unless ZA and ZB lie on the same segment). The following equations are used in cards 310 - 319 to evaluate the subintegral on segment I:

$$(80) \qquad \int_{h_a}^{h_b} \underline{A}(g) \cos g \, dg = \frac{1}{DG} \left[CI \, \underline{A}(I) + CII \, \underline{A}(I+1) \right] ,$$

$$(81) \qquad \int_{h_a}^{h_b} \underline{A}(g) \sin g \, dg = \frac{1}{DG} \left[DI \, \underline{A}(I) + DII \, \underline{A}(I+1) \right] ,$$

$$(82) \qquad CI = (h_a - g_{i+1}) \sin h_a + (g_{i+1} - h_b) \sin h_b + \cos h_a - \cos h_b \quad ,$$

$$(83) \qquad CII = (g_i - h_a) \sin h_a + (h_b - g_i) \sin h_b + \cos h_b - \cos h_a \quad ,$$

$$(84) \qquad DI = (g_{i+1} - h_a) \cos h_a + (h_b - g_{i+1}) \cos h_b + \sin h_a - \sin h_b \quad ,$$

and

$$(85) \qquad DII = (h_a - g_i)\cos h_a + (g_i - h_b)\cos h_b + \sin h_b - \sin h_a \ .$$

DG is defined in Eq. (59). In the program, g_i, g_{i+1}, h_a and h_b are denoted by G, GP, HA and HB. SGN is positive in the first pass through this integration loop and negative in the second pass, in accordance with the plus and minus signs in Eqs. (78) and (79).

When the vectors $\underline{U}(t)$ and $\underline{V}(t)$ have been calculated, Eq. (68) is used to determine $\underline{F}(t)$. The rectangular components of $\underline{F}(t)$ are denoted by FX, FY and FZ in cards 330-332. Finally cards 333 - 336 calculate the scattering functions defined by Eqs. (43) through (47), and card 337 arranges the writeout of these data on the scattering waveforms for the pulse situation.

The results obtained in this manner (using the input data in Fig. 1) for a prolate spheroid are illustrated in Fig. 8.

VIII. CONCLUSIONS

A digital computer program is described which uses the physical optics approximation for scattering by convex perfectly conducting targets with arbitrary shape. The target size and shape are specified by input data giving the coordinates of many points on the surface. This program handles bistatic and backscatter problems. The input data specify the frequency, the incidence angles (θ_i, ϕ_i) and the scattering angles (θ_s, ϕ_s). In the CW case, the output data give the complex elements in the scattering matrix. Typical results are shown in the Appendix for scattering from spheres, spheroids, ogives and cones.

This scattering program also handles the pulse case where the incident wave has a finite number of cycles. For this case, the following additional input data are required: the number of cycles in the incident wavetrain, and the number of points per cycle to be computed for the scattering waveforms. The output data give the four waveforms associated with the four elements in the scattering matrix.

Simple modifications can be made in the program, if desired, to increment the frequency, the incidence angles or the scattering angles. This is convenient for generating various types of scattering curves such as those in the Appendix.

```
    4 CONTINUE
      LM=L*M
      FL=L
      FM=M
      WTAU=TP*FM
      DWT=TP/FL
      IF(LM.EQ.0)GO TO 300
      DGT=TPL*DELT
      G1=TPL*WI
      GX=TPL*WMAX
      GN=TPL*WMIN
      DEN=TP*DG
      WTA=-GX
      WTB=WTAU-GN
      WT=WTA
      F11=0.0
      F12=0.0
      F21=0.0
      F22=0.0
      WRITE(6,22) WT,F11,F12,F21,F22
      UX=.0
      UY=.0
      UZ=.0
      VX=.0
      VY=.0
      VZ=.0
      XB=GX
      YB=GX
  260 WT=WT+DWT
      IF(WT.GT.WTB) GO TO 300
      SWT=SIN(WT)
      CWT=COS(WT)
      XA=GN
      KA=1
      XX=-WT
      IF(XX.LE.XA) GO TO 265
      XA=XX
      KA=(XA-G1)/DG+1.5
  265 YA=GX
      LA=KX
      YY=WTAU-WT
      IF(YY.GE.YA) GO TO 268
      YA=YY
      LA=(YA-G1)/DG+1.5
  268 SGN=1.
      ZA=XA
      ZB=XB
      I=KA
      F=I-1
      G=F*DG+G1
      DO 290 K=1,2
      IF(ZA.GE.ZB) GO TO 285
  270 GP=G+DG
      HA=G-DGT
      HB=G+DGT
      IF(HA.LT.ZA) HA=ZA
      IF(HB.GT.ZB) HB=ZB
      SA=SIN(HA)
      SB=SIN(HB)
      CA=COS(HA)
      CB=COS(HB)
      C1=(SA*(HA-GP)+SB*(GP-HB)+CA-CB)*SGN
```

Fig. 7. Last section of the computer program.

```
      CII=(SA*(G-HA)+SB*(HB-G)+CB-CA)*SGN
      UX=UX+CI*AX(I)+CII*AX(I+1)
      UY=UY+CI*AY(I)+CII*AY(I+1)
      UZ=UZ+CI*AZ(I)+CII*AZ(I+1)
      DI=(SA-SB+CA*(GP-HA)+CB*(HB-GP))*SGN
      DII=(SB-SA+CA*(HA-G)+CB*(G-HB))*SGN
      VX=VX+DI*AX(I)+DII*AX(I+1)
      VY=VY+DI*AY(I)+DII*AY(I+1)
      VZ=VZ+DI*AZ(I)+DII*AZ(I+1)
      IF(HB.GE.ZB) GO TO 285
      I=I+1
      G=GP
      GO TO 270
  285 ZA=YA
      ZB=YB
      I=LA
      F=I-1
      G=F*DG+GI
  290 SGN=-1.
      FX=(UX*CWT-VX*SWT)/DEN
      FY=(UY*CWT-VY*SWT)/DEN
      FZ=(UZ*CWT-VZ*SWT)/DEN
      F11=FX*X11+FY*Y11+FZ*Z11
      F12=FX*X12+FY*Y12+FZ*Z12
      F21=FZ*Z21
      F22=FX*X22+FY*Y22+FZ*Z22
      WRITE(6,22) WT,F11,F12,F21,F22
      XB=XA
      YB=YA
      GO TO 260
  300 CONTINUE
      WRITE (6,23)
      STOP
      END
$DATA
```

Fig. 7. Last section of the computer program. (cont.)

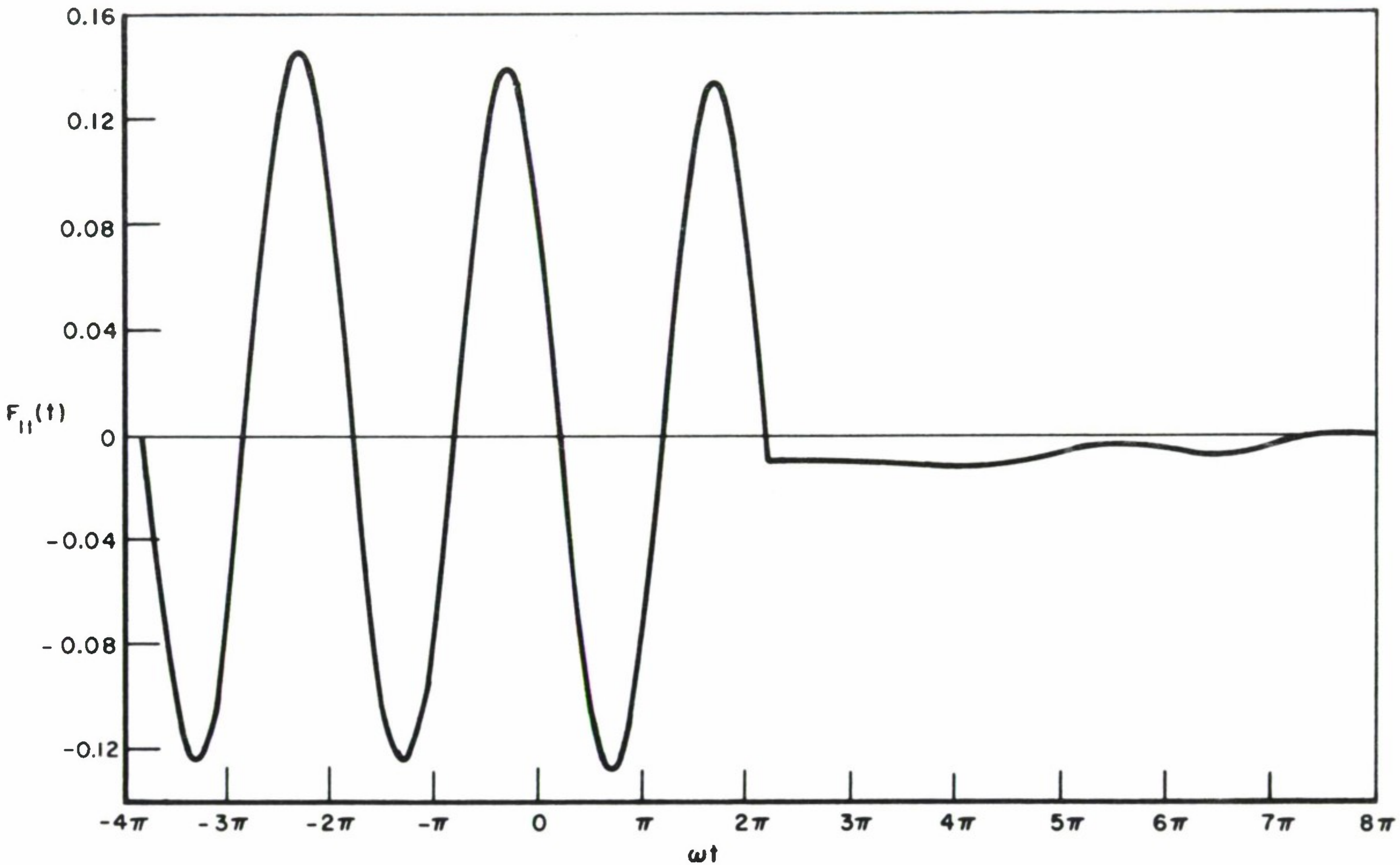

Fig. 8. Calculated pulse response for prolate spheroid, using input data from Fig. 1.

REFERENCES

1. Richmond, J.H., "The Numerical Evaluation of Radiation Integrals," IRE Transactions, Vol. AP-9, (July 1961), pp. 358-360.

2. Siegel, K.M., et al, "Studies in Radar Cross-Sections VIII - Theoretical Cross-Sections as a Function of Separation Angle Between Transmitter and Receiver at Small Wavelengths," UMM-115, Willow Run Research Center, University of Michigan, (October 1953).

APPENDIX
NUMERICAL RESULTS

This Appendix presents the results obtained with the physical-optics computer program for several target shapes. Table I lists the number of planes used to describe each target, the total number of points on the target, and the time required for an IBM 7094 to process the target description data and set up the polyhedral approximation. The last column lists the additional computer time needed to calculate the area function and the CW scattering matrix.

TABLE I
STATISTICS FOR THE TEST CASES

Target Shape	Planes	Points	Time for Polyhedron	Area Function and CW Matrix
Sphere	30	1083	8.6 sec	1.6 sec
Prolate Spheroid	30	774	6.4	1.3
Oblate Spheriod	30	1257	9.9	1.9
Ogive	50	1008	8.2	1.8
Cone	35	1176	9.8	3.3

The dimensions of the targets are specified in Figs. 9 through 13.

It is found from Table I that the computation time for processing the target description data and setting up the polyhedron increases linearly with the number of points on the target surface. The computer handles about 125 points (to establish 250 facets) per second, regardless of the shape of the target.

In generating the area function and the CW scattering matrix, the computer spends very little time on the shadowed facets. Thus, the computation time for this work increases linearly with the number of illuminated facets on the target. This explains why the computer spent twice as much time on the cone (3.3 seconds) as on the sphere (1.6 seconds) as shown in Table I This sphere has approximately 2000 facets, and half of them are illuminated. The cone also has approximately 2000 facets, and all of them are illuminated for axial incidence.*

In calculating the area function, the computer handles about 670 illuminated facets per second.

To use the computer program most efficiently, one would calculate a significant amount of scattering data for one target before passing on to the next one. Furthermore, to minimize the area-function calculations, one would calculate the scattering data for many different frequencies before changing θ_i, ϕ_i, θ_s or ϕ_s. When these incidence and scattering angles are held constant, the computer generates CW scattering data for 20 different frequencies in one second for the oblate spheroid in Table I, and for 10 frequencies per second for the cone. For the sphere, it generates CW and pulse-response data for a new frequency in one second (with three cycles in the incident wavetrain and 20 calculated points per cycle in the scattering waveform).

Figures 9 through 13 display the numerical results for scattering by several different target shapes. The dots represent the output data from the computer program described herein. The input data listed the coordinates of a large number of points (Table I) distributed almost uniformly over the target surface. The source of the physical-optics data (the solid curves in Figs. 9 - 13) is described a little farther on in this Appendix.

Figures 9a through 13a show curves of backscatter echo area (in square meters) versus frequency for axial incidence. For each of these targets, it may be noted that the computer output agrees closely with the physical optics solution for all frequencies up to 600 MHz. (This simply indicates that the computer program does a good job in generating physical optics data. It is not implied that the physical optics formulation always gives a good approximation to the exact scattering data.) To obtain equally good results at higher frequencies, it would be necessary to include more points in the input data description of the target.

---

* For all the targets listed in Table I except the cone, the input data points covered the whole surface and the computer set up a closed polyhedron. For the cone, however, the input data did not cover the flat plate at the base. Since the base is shadowed for all cases shown in Fig. 13, the computed data apply to a cone with a circular disk at the base.

Although the computer program has not been adequately tested for the most general target shapes and bistatic situations for which it is designed, it is believed that it will give accurate physical-optics data except for concave targets, forward scattering, and specular scattering from a large flat subsurface. The program could be modified without much difficulty to remove the last two of these exceptions.

All of the targets considered in this Appendix have axial symmetry with respect to the z axis. To check the accuracy of the computer output data shown in Figs. 9a - 13a, closed-form expressions were derived for the vector area function for each of these targets for the backscatter situations with axial incidence. Letting $\theta_i = \phi_i = \theta_s = \phi_s = 0$, we find from Eq. (22) that $w = 2z$. From symmetry considerations, $A_x(w) = A_y(w) = 0$. For targets having axial symmetry with respect to the z axis, it is convenient to describe the target shape with an equation of the form $\rho = \rho(z)$ where (ρ, ϕ, z) represent the coordinates in the cylindrical system. Then it is easy to show, with the aid of Eq. (51), that

$$(84) \qquad A_z(w) = -\pi \rho \rho' \quad ,$$

where ρ' represents the derivative of $\rho(z)$ with respect to z. Equation (84) applies over the illuminated region of the target where ρ' is negative, and $A_z(w) = 0$ over the shadowed region where ρ' is positive.

All the targets considered in this Appendix can be represented with the following equation:

$$(85) \qquad F(\rho, z) = A_1 \rho^2 + A_2 z^2 + A_3 \rho z + A_4 z + A_5 \rho + A_6 = 0 \ .$$

From Eqs. (84) and (85), the area function for axial backscatter is given in closed form by

$$(86) \qquad A_z = \pi \rho (2A_2 z + A_3 \rho + A_4)/(2A_1 \rho + A_3 z + A_5) \ .$$

For spheres, prolate spheroids and oblate spheroids,

(87) $$A_z = \frac{\pi z B^2}{A^2}$$

where A and B denote the semimajor and semiminor axes, respectively. For the ogive,

(88) $$A_z = \frac{\pi \rho z}{\sqrt{B^2 - z^2}} \quad ,$$

where B is the radius of the circular are that generates the ogive.

For the cone,

(89) $$A_z = \pi z \tan^2 \alpha \quad ,$$

where α denotes the half-angle of the cone.

For axial backscatter from a target with axial symmetry, it is found from Eq. (54) that $S_x = S_y = 0$ and

(90) $$S_z = (2j/\lambda) \int A_z \, e^{2jkz} \, dz \ .$$

The integral in Eq. (90) can be evaluated to obtain closed-form expressions for the scattering matrix and the echo area for the cone and the spheroids. The resulting data are shown by the solid curves with the label "physical optics" in Figs. 9a, 10a, 11a and 13a. For the ogive in Fig. 12a, the "physical optics" curve was obtained from Eqs. (88) and (90) with numerical integration.

Figure 9b shows backscatter results for the sphere as a function of the aspect angle. For a true sphere, the echo area is of course independent of aspect angle. Thus, the variations in the computer output data arise from the polyhedral approximation.

Figures 10b - 13b show the backscatter results as a function of the aspect angle ($\theta_i = \theta_s = \theta$) for the spheroids, ogive and cone. The solid curves with the label "physical optics" were obtained with another computer program which is designed especially for backscattering from targets with axial symmetry. The input data for this auxiliary program describes the target shape by assigning numerical values to the coefficients in Eq. (85). The angles ϕ_i and ϕ_s are assumed to be zero, the cylindrical coordinates (ρ, ϕ, z) are employed for points on the target surface, and

(91) $$w = 2(\rho \sin\theta \cos\phi + z \cos\theta).$$

It is found that $S_y = 0$,

(92) $$\underline{S} = (j/\lambda) \int\int (\hat{x} \cos\phi - \hat{z}\, \rho') \rho\, e^{jkw}\, d\phi\, dz ,$$

(93) $$S_{11} = S_{22} = - S_x \sin\theta - S_z \cos\theta ,$$

and $S_{12} = S_{21} = 0$. The auxiliary program uses numerical integration to evaluate $\underline{S}$ in Eq. (92).

Bistatic scattering results are shown in Figs. 9c - 13c and 9d - 13d. These curves apply for axial incidence with $\theta_i = \phi_i = \phi_s = 0$, so that

(94) $$w = \rho \sin\theta_s \cos\phi + z(1 + \cos\theta_s) ,$$

(95) $$S_x = - k \int \rho\, J_1(k \rho \sin\theta_s)\, e^{jkz(1+\cos\theta_s)}\, dz ,$$

(96) $$S_y = S_{12} = S_{21} = 0 ,$$

(97) $$S_z = - jk \int \rho\, \rho'\, J_o(k \rho \sin\theta_s)\, e^{jkz(1+\cos\theta_s)}\, dz ,$$

(98) $$S_{11} = - S_x \sin\theta_s - S_z \cos\theta_s ,$$

(99) $$S_{22} = - S_z ,$$

and J_o and J_1 represent Bessel functions.

Equations (94) - (99) apply only for axial incidence on a target having axial symmetry. (Similar expressions are given in Reference 2.) These equations were used to develop another auxiliary computer program to generate the E-plane and H-plane curves with the label "physical optics". This program also used the coefficients in Eq. (85) as input data for the target shape, and evaluated S_x and S_z with numerical integration.

The bistatic curves in Figs. 9 - 13 agree with the physical-optics echo area expression for the forward-scattering situation:

(100) $$\sigma = 4\pi A^2/\lambda^2 \quad ,$$

where A represents the area of the target projected along the line of sight between the transmitting and receiving antennas. In the forward-scattering situation (and also for backscattering), the physical optics echo area shows no polarization dependence even for a target with arbitrary shape. Equation (100) is not restricted to symmetrical targets or axial incidence.

Though <u>all</u> the data in Figs. 9 - 13 were obtained with the aid of various digital computer programs based on the physical-optics concepts, the close agreement between the dots (with the label "computer output") and the curves (with the label "physical optics") is significant for two reasons. First, the general program uses a target description technique which differs greatly from that used in the specialized programs. Furthermore, some of the specialized programs used closed-form expressions and others were based on equations involving line integrals or surface integrals, whereas the general program handles each problem in the same manner (setting up the polyhedron, calculating the vector area function, and integrating the area function to obtain the scattering matrix). Having demonstrated that this general procedure gives correct physical-optics data for a variety of target shapes and bistatic and backscatter situations, we have confidence that the program will perform equally well with other targets and situations.

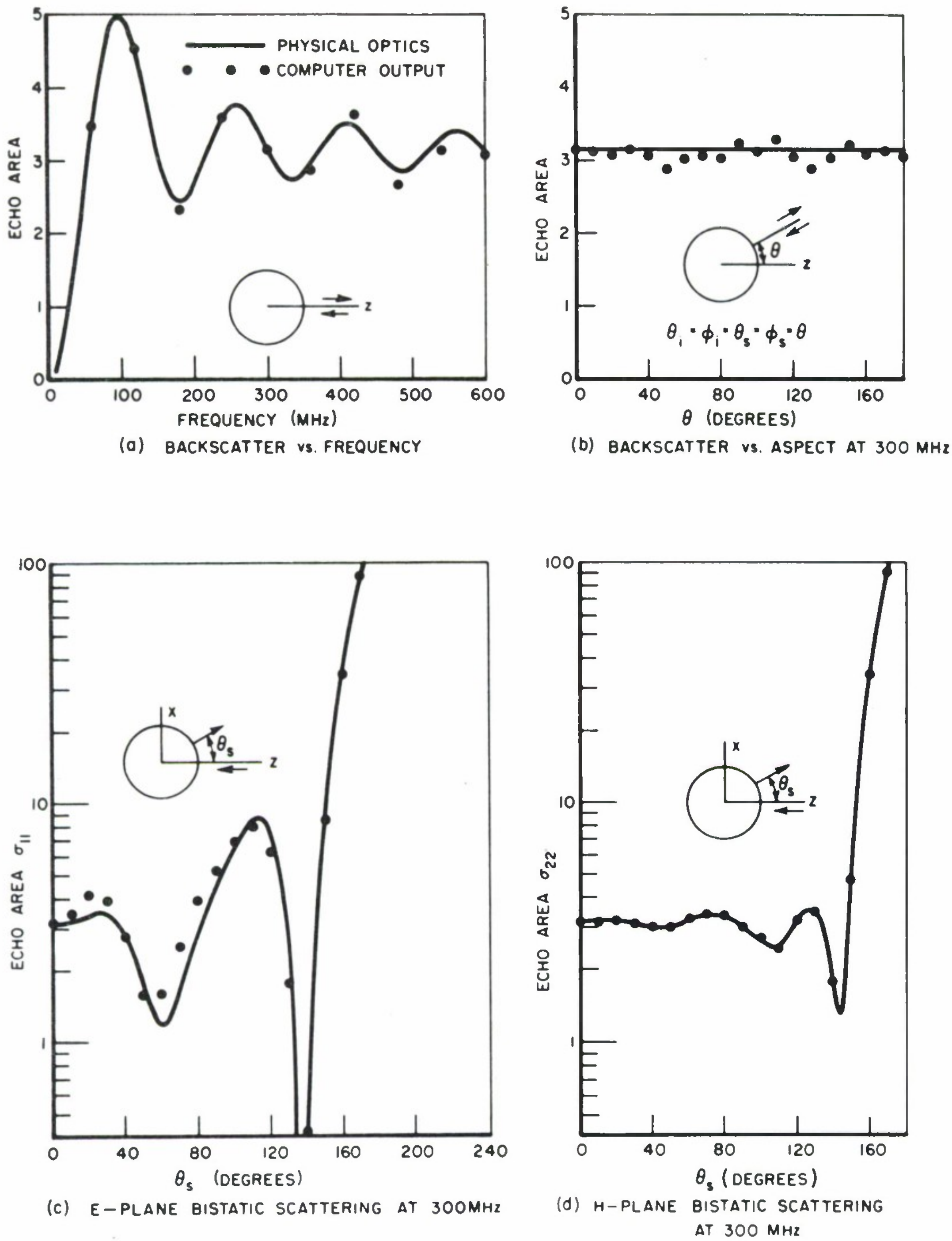

Fig. 9. Scattering data for a sphere with a radius of one meter.

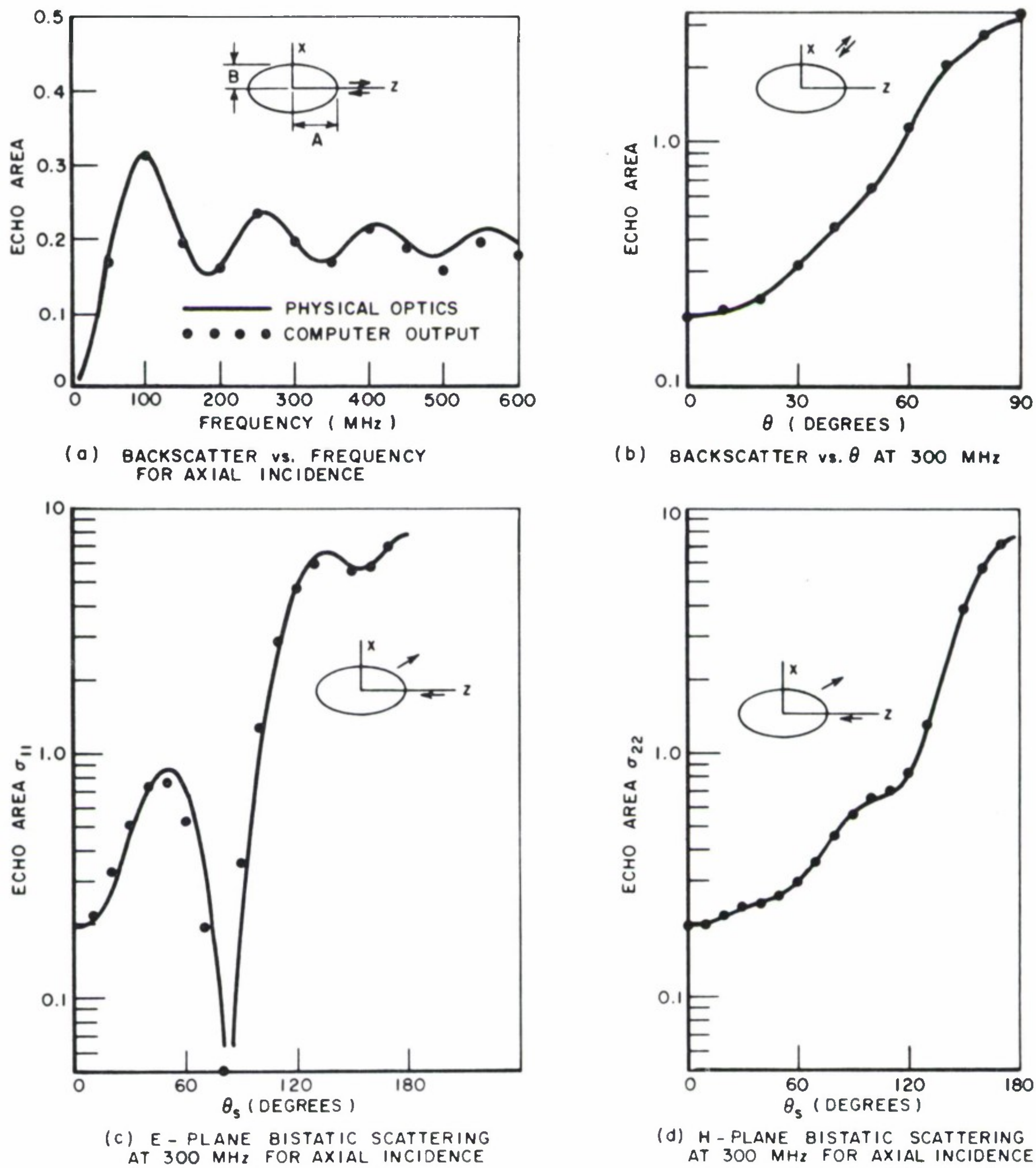

Fig. 10. Scattering data for a prolate spheroid with A = 1 m and B = 0.5 m.

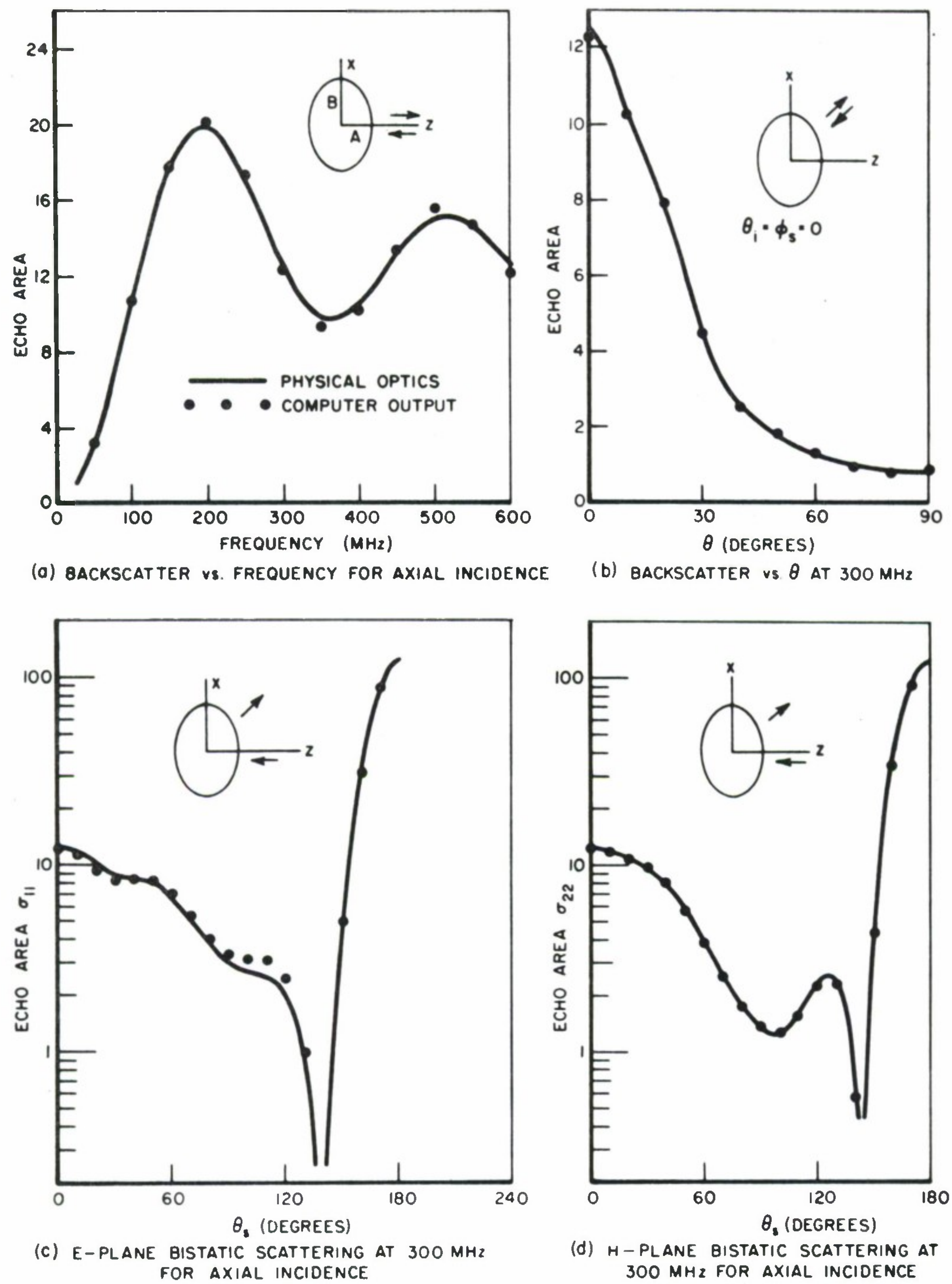

Fig. 11. Scattering data for an oblate spheroid with A = 0.5 m and B = 1 m.

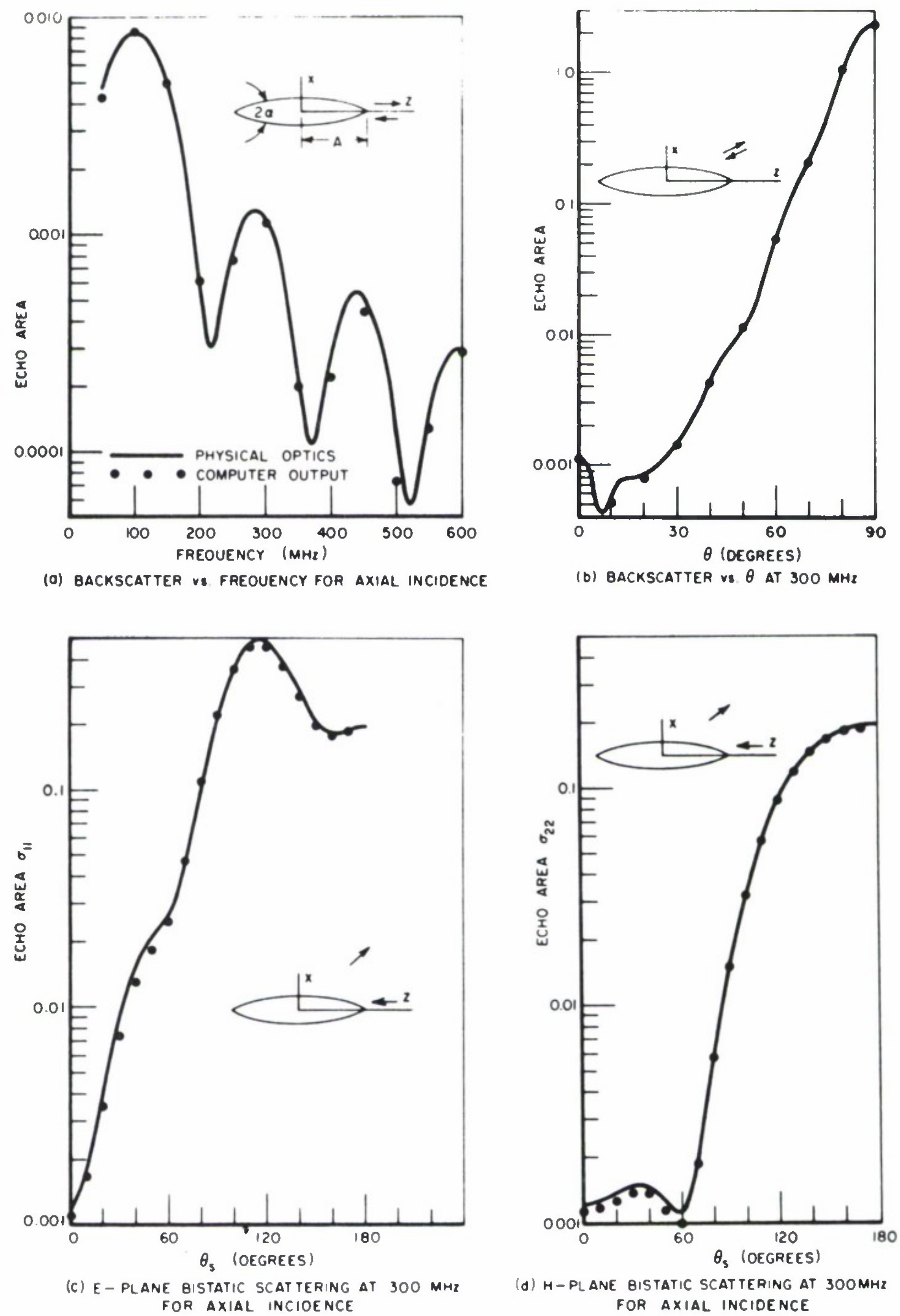

Fig. 12. Scattering data for an ogive with $A = 1$ m and $\alpha = 22.5°$.

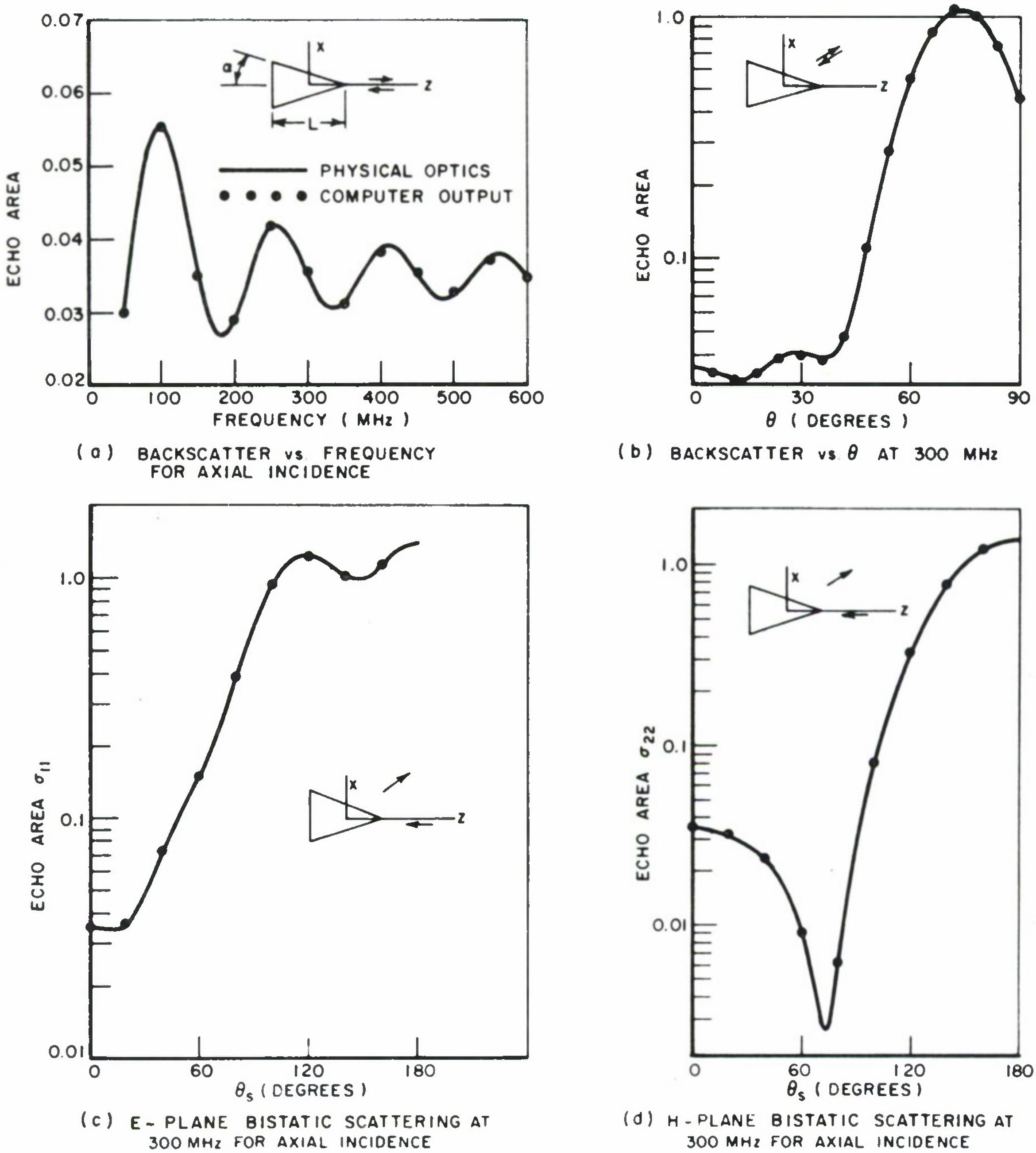

Fig. 13. Scattering data for a cone with
L = 1 m and α = 18°.

UNCLASSIFIED
Security Classification

DOCUMENT CONTROL DATA - R&D

(Security classification of title, body of abstract and indexing annotation must be entered when the overall report is classified)

1. ORIGINATING ACTIVITY *(Corporate author)* The Ohio State University, ElectroScience Laboratory Department of Electrical Engineering 1320 Kinnear Road, Columbus, Ohio	2a. REPORT SECURITY CLASSIFICATION Unclassified 2b. GROUP N/A

3. REPORT TITLE
A Computer Program for Physical-Optics Scattering by Convex Conducting Targets

4. DESCRIPTIVE NOTES *(Type of report and inclusive dates)*
Technical Report

5. AUTHOR(S) *(Last name, first name, initial)*
Richmond, Jack H.

6. REPORT DATE	7a. TOTAL NO. OF PAGES	7b. NO. OF REFS
May 1968	42	2

8a. CONTRACT OR GRANT NO. F-19628-67-C-0308 b. PROJECT NO. c. TASK d.	9a. ORIGINATOR'S REPORT NUMBER(S) ESD-TR-68-216 9b. OTHER REPORT NO(S) *(Any other numbers that may be assigned this report)*

10. AVAILABILITY/LIMITATION NOTICES
This document has been approved for public release and sale; its distribution is unlimited

11. SUPPLEMENTARY NOTES	12. SPONSORING MILITARY ACTIVITY Deputy for Surveillance and Control Systems, Electronic Systems Div. L.G. Hanscom Field, Bedford, Mass.

13. ABSTRACT

This report describes a digital computer program which uses the physical optics approximation to calculate the scattering properties of convex perfectly conducting targets with arbitrary shape. The target shape is described in terms of the coordinates of a large number of points on the surface.

The program handles bistatic as well as backscattering problems. The input data specify the frequency, the incidence angles (θ_i, ϕ_i) and the scattering angles (θ_s, ϕ_s). In the CW case, the output data give the complex elements in the scattering matrix.

The program also handles the pulse case where the incident waveform has a finite number of cycles.

Graphs are included to illustrate typical results for the following target shapes: sphere, spheroids, ogive, and cone.

DD FORM 1473 1 JAN 64

UNCLASSIFIED
Security Classification

UNCLASSIFIED
Security Classification

14. KEY WORDS	LINK A		LINK B		LINK C	
	ROLE	WT	ROLE	WT	ROLE	WT
Radar cross section Backscatter Bistatic scattering Physical optics Digital computation Pulse response						

INSTRUCTIONS

1. ORIGINATING ACTIVITY: Enter the name and address of the contractor, subcontractor, grantee, Department of Defense activity or other organization *(corporate author)* issuing the report.

2a. REPORT SECURITY CLASSIFICATION: Enter the overall security classification of the report. Indicate whether "Restricted Data" is included. Marking is to be in accordance with appropriate security regulations.

2b. GROUP: Automatic downgrading is specified in DoD Directive 5200.10 and Armed Forces Industrial Manual. Enter the group number. Also, when applicable, show that optional markings have been used for Group 3 and Group 4 as authorized.

3. REPORT TITLE: Enter the complete report title in all capital letters. Titles in all cases should be unclassified. If a meaningful title cannot be selected without classification, show title classification in all capitals in parenthesis immediately following the title.

4. DESCRIPTIVE NOTES: If appropriate, enter the type of report, e.g., interim, progress, summary, annual, or final. Give the inclusive dates when a specific reporting period is covered.

5. AUTHOR(S): Enter the name(s) of author(s) as shown on or in the report. Enter last name, first name, middle initial. If military, show rank and branch of service. The name of the principal author is an absolute minimum requirement.

6. REPORT DATE: Enter the date of the report as day, month, year, or month, year. If more than one date appears on the report, use date of publication.

7a. TOTAL NUMBER OF PAGES: The total page count should follow normal pagination procedures, i.e., enter the number of pages containing information.

7b. NUMBER OF REFERENCES: Enter the total number of references cited in the report.

8a. CONTRACT OR GRANT NUMBER: If appropriate, enter the applicable number of the contract or grant under which the report was written.

8b, 8c, & 8d. PROJECT NUMBER: Enter the appropriate military department identification, such as project number, subproject number, system numbers, task number, etc.

9a. ORIGINATOR'S REPORT NUMBER(S): Enter the official report number by which the document will be identified and controlled by the originating activity. This number must be unique to this report.

9b. OTHER REPORT NUMBER(S): If the report has been assigned any other report numbers *(either by the originator or by the sponsor)*, also enter this number(s).

10. AVAILABILITY/LIMITATION NOTICES: Enter any limitations on further dissemination of the report, other than those imposed by security classification, using standard statements such as:

(1) "Qualified requesters may obtain copies of this report from DDC."

(2) "Foreign announcement and dissemination of this report by DDC is not authorized."

(3) "U. S. Government agencies may obtain copies of this report directly from DDC. Other qualified DDC users shall request through
___________________________________."

(4) "U. S. military agencies may obtain copies of this report directly from DDC. Other qualified users shall request through
___________________________________."

(5) "All distribution of this report is controlled. Qualified DDC users shall request through
___________________________________."

If the report has been furnished to the Office of Technical Services, Department of Commerce, for sale to the public, indicate this fact and enter the price, if known.

11. SUPPLEMENTARY NOTES: Use for additional explanatory notes.

12. SPONSORING MILITARY ACTIVITY: Enter the name of the departmental project office or laboratory sponsoring *(paying for)* the research and development. Include address.

13. ABSTRACT: Enter an abstract giving a brief and factual summary of the document indicative of the report, even though it may also appear elsewhere in the body of the technical report. If additional space is required, a continuation sheet shall be attached.

It is highly desirable that the abstract of classified reports be unclassified. Each paragraph of the abstract shall end with an indication of the military security classification of the information in the paragraph, represented as *(TS)*, *(S)*, *(C)*, or *(U)*.

There is no limitation on the length of the abstract. However, the suggested length is from 150 to 225 words.

14. KEY WORDS: Key words are technically meaningful terms or short phrases that characterize a report and may be used as index entries for cataloging the report. Key words must be selected so that no security classification is required. Identifiers, such as equipment model designation, trade name, military project code name, geographic location, may be used as key words but will be followed by an indication of technical context. The assignment of links, rules, and weights is optional.

UNCLASSIFIED
Security Classification